Journal of Materials, Processes and Environment
May edition. Vol. 5. N° 1. (2017)
ISSN : 2335-1020

Thermal Stability Of FGM Rectangular Plates Using A New Hyperbolic Shear Deformation Theory

Chikh Abdelbaki[1,2], Tounsi. A[1,3], Adda Bedia E. A[1,3]

1. Laboratoire des Matériaux et Hydrologie, Université de Sidi Bel Abbes, Algérie.
2. Département de génie civil, Faculté des sciences appliquées, Université Ibn Khaldoun de Tiaret, Algérie
3. Département de génie civil et travaux publics, Faculté de technologie, Université de Sidi Bel Abbes, Algérie

ABSTRACT — In this paper, a new hyperbolic shear deformation beam theory is developed, the study of thermal buckling analysis of plates functionally graded material (FGM) resting on elastic foundations. The equilibrium equations of the FGM plate are based on the high order hyperbolic shear deformation theory and includes the plate-foundation interaction and thermal effects. Material properties vary depending on the form of the power law through the thickness (P-FGM). The governing equations are solved analytically for a plate with simply supported boundary conditions and submitted through its thickness uniform temperature gradient, linear and nonlinear. The resulting equations are used to obtain the exact solution for the critical buckling load for each load. The influences of the aspect ratio of the plate, the side-to-thickness ratio, the rigidity of the elastic foundation on the buckling temperature difference are discussed.

***Keywords**: functionally graded materials, Hyperbolic shear deformation theory, Pasternak elastic foundation.*

I.Introduction

Functionally graduated equipment (FG) is relatively a new technology used in components subjected to high temperature. Laminated composite materials allow design flexibility to achieve desirable stiffness and strength through the choice of laminating system, laminated composite structures typically subjected to stress concentrations and due to discontinuities in the characteristics, material failures observed in laminated composites in the form of peeling, matrix cracking, and bonding separation. FGM can withstand such problems because of continuous change in material characteristics from one surface to another, particularly through thickness.

Plates resting on elastic foundation are important in structural engineering and have wide application in other fields of engineering. Such plate structures can be found in various types of industrial applications such as rafters, storage tanks, swimming pools, and in most civil engineering constructions. Models with one and two parameters for the soil under the plate are introduced to model the foundation. The Pasternak model or the two-parameter model is widely adopted to describe the mechanical behavior of foundations, and the well-known Winkler model is one of its particular cases. Indeed, two-parameter elastic base models have been developed to overcome Winkler's inadequacy model to describe the real soil reaction and the mathematical complexity of the three-dimensional continuous. The two-parameter model (Pasternak model) estimates the shear deformation between the springs on the model of a parameter, while the one-parameter model (Winkler model) can be represented by continuous springs. Therefore, the Winkler model can be considered as a special case of the Pasternak model by setting the shear modulus to zero.

***Corresponding author**: Chikh Abdelbaki Département de génie civil, Faculté des sciences appliquées, Université Ibn Khaldoun de Tiaret, ALGÉRIE*
Email : cheikhabdelbakki@yahoo.fr,

The first order shear deformation theory is used by Wu [1] to determine the analytical expressions of critical buckling temperatures for simply supported FGM plates. Woo et al. [2] used a Fourier series mixed solution to obtain analytical solutions to study the post-buckling response of moderately thick and shallow FGM plates under compression load and specified temperature field. Prakash et al. [3] used a quadrilateral plate element to examine the pseudo-post-buckling non-linear flexural response of functionally graded plates based on the first-order deformation theory in order to shear under thermomechanical loading. Matsunaga [4] proposed a 2D global theory of higher order deformation for functionally graduated thermal plate buckling. He calculated the critical buckling temperatures of a functionally graduated plate simply supported under uniformly and linearly distributed temperatures.

Thus, these new materials are selected, we can be used in structural elements of aircraft, aerospace vehicles, nuclear power plants as well as various high temperature structures often used in industries (Shahrjerdi et al [5], Tounsi et al , Bouidba et al, [7] Golmakani, [8] Chakraverty and Pradhan, [9,10], Zidi et al, [11] Belabed et al, [12] Bousahla et al, 13], Hebali et al, [14], Mantari and Granados [15], Pradhan, KK and Chakraverty, S. [16] Rad, [17] Mahi et al.

In the present paper, an analytical solution for the static response of functionally graded thick plates (FGM) based on elastic foundations (of the Pasternak type) is developed using a high order hyperbolic shear deformation theory recently by Abdelbaki Chikh et al. [19].

The results obtained by this theory are compared with those determined by high order theories. The influence of several parameters on the response to buckling of functionally graduated plates (FGM) based on elastic foundations is discussed in detail

II. The Properties Of FGM Plate Materials

In this parer, a rectangular P-FGM plate made with functionally graduated ceramic and metal materials. A coordinate system (x,y,z) is considered in which (x,y) is the median plane of the plate and z is the thickness direction (-h/2≤z≤h/2) as shown in Fig. III. 1.

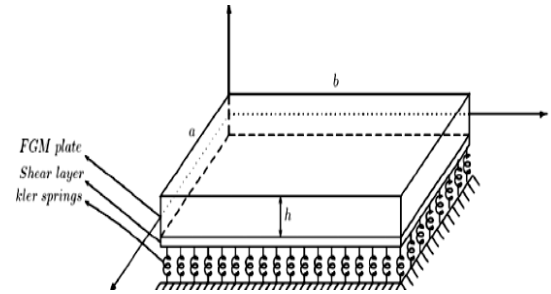

Fig. 1: P-FGM plate on an elastic foundation.

The material properties P of the P-FG plate such as the modulus of elasticity E and the coefficient of thermal expansion α vary in the direction of thickness z in accordance with the linear mixing law as:

$$P(z) = P_m + (P_c - P_m)\left(\frac{2z+h}{2h}\right)^P \quad (1)$$

Where Pm and Pc are the corresponding properties of the metal and ceramic, respectively. The volume fractions of metal and ceramic, and it is assumed that:

$$V(z) = \left(\frac{z}{h} + \frac{1}{2}\right)^P \quad (2)$$

Where:

P: is the index of power law which takes the values plus or equal to zero.

III. Theoretical Formulations

Based on a new hyperbolic theory of shear deformation, the following displacement field is assumed:

$$u(x,y,z) = u_0(x,y) - z\frac{\partial w_b(x,y)}{\partial x} - f(z)\frac{\partial w_s(x,y)}{\partial x} \quad (3a)$$

$$v(x,y,z) = v_0(x,y) - z\frac{\partial w_b(x,y)}{\partial y} - f(z)\frac{\partial w_s(x,y)}{\partial y} \quad (3b)$$

$$w(x,y,z) = w_b(x,y) + w_s(x,y) \quad (3c)$$

With: u_0, v_0, w_b, w_s are four displacements unknown to the median plane of the plate.

I.1.The different theories of plates

The classical plate theory (CPT): $f(z) = 0$

First order shears deformation theory (FSDT): $f(z) = z$

Third order shears deformation theory (TSDT): $f(z) = z\left(1 - \frac{4z^2}{3h^2}\right)$

The sinusoidal shear deformation theory (SSDT): $f(z) = \frac{h}{\pi} sin\left(\frac{\pi z}{h}\right)$

The present theory is given by (Abdelbaki Chikh et al [19]):

$$f(z) = \frac{1}{10}\left(\frac{h \sinh\left(10\frac{z}{h}\right)}{\cosh(5)}\right) + \frac{h}{100}$$

The deformation-displacement equations are the following:

$$\begin{Bmatrix} \varepsilon_x \\ \varepsilon_y \\ \gamma_{xy} \end{Bmatrix} = \begin{Bmatrix} \varepsilon_x^0 \\ \varepsilon_y^0 \\ \gamma_{xy}^0 \end{Bmatrix} + z\begin{Bmatrix} k_x^b \\ k_y^b \\ k_{xy}^b \end{Bmatrix} + f(z)\begin{Bmatrix} k_x^s \\ k_y^s \\ k_{xy}^s \end{Bmatrix},$$

$$\begin{Bmatrix} \gamma_{yz} \\ \gamma_{xz} \end{Bmatrix} = g(z)\begin{Bmatrix} \gamma_{yz}^s \\ \gamma_{xz}^s \end{Bmatrix} \quad (4)$$

With:

$$\begin{Bmatrix} \varepsilon_x^0 \\ \varepsilon_y^0 \\ \gamma_{xy}^0 \end{Bmatrix} = \begin{Bmatrix} \frac{\partial u_0}{\partial x} \\ \frac{\partial v_0}{\partial x} \\ \frac{\partial u_0}{\partial y} + \frac{\partial v_0}{\partial x} \end{Bmatrix}, \quad \begin{Bmatrix} k_x^b \\ k_y^b \\ k_{xy}^b \end{Bmatrix} = \begin{Bmatrix} -\frac{\partial^2 w_b}{\partial x^2} \\ -\frac{\partial^2 w_b}{\partial y^2} \\ -2\frac{\partial^2 w_b}{\partial x \partial y} \end{Bmatrix},$$

$$\begin{Bmatrix} k_x^s \\ k_y^s \\ k_{xy}^s \end{Bmatrix} = \begin{Bmatrix} -\frac{\partial^2 w_s}{\partial x^2} \\ -\frac{\partial^2 w_s}{\partial y^2} \\ -2\frac{\partial^2 w_s}{\partial x \partial y} \end{Bmatrix}, \quad \begin{Bmatrix} \gamma_{yz}^s \\ \gamma_{xz}^s \end{Bmatrix} = \begin{Bmatrix} \frac{\partial w_s}{\partial y} \\ \frac{\partial w_s}{\partial x} \end{Bmatrix} \quad (5)$$

And:

$$g(z) = 1 - \frac{df(z)}{dz} \quad (6)$$

The linear constitutive relations of a P-FG plate can be expressed as:

$$\begin{Bmatrix} \sigma_x \\ \sigma_y \\ \tau_{xy} \\ \tau_{yz} \\ \tau_{xz} \end{Bmatrix} = \begin{bmatrix} Q_{11} & Q_{12} & 0 & 0 & 0 \\ Q_{12} & Q_{22} & 0 & 0 & 0 \\ 0 & 0 & Q_{66} & 0 & 0 \\ 0 & 0 & 0 & Q_{44} & 0 \\ 0 & 0 & 0 & 0 & Q_{55} \end{bmatrix} \begin{Bmatrix} \varepsilon_x - \alpha\Delta T \\ \varepsilon_y - \alpha\Delta T \\ \gamma_{xy} \\ \gamma_{yz} \\ \gamma_{xz} \end{Bmatrix} \quad (7)$$

Or ΔT is the temperature difference between the two surfaces of the P-FGM plate.

Where: $(\sigma_{xx}, \sigma_{yy}, \tau_{xy}, \tau_{yz}, \tau_{yx})$ and $(\varepsilon_{xx}, \varepsilon_{yy}, \gamma_{xy}, \gamma_{yz}, \gamma_{yx})$ are the terms of stresses and deformations, respectively.

The stiffness coefficients can be expressed as:

$$Q_{11} = Q_{22} = \frac{E(z)}{1-\nu^2} \quad (8)$$

$$Q_{12} = \frac{\nu E(z)}{1-\nu^2} \quad (9)$$

$$Q_{44} = Q_{55} = Q_{33} = \frac{E(z)}{2(1+\nu)} \quad (10)$$

IV. The equilibrium equations

By using the virtual work principle to minimize the functional result of the total potential energy function in the expressions of nonlinear equilibrium equations of a P-FGM plate based on two parameters of the elastic foundations.

The principle of virtual works in this case expressed by:

$$\int_{-h/2}^{h/2}\int_{\Omega}\left[\sigma_{xx}\delta\varepsilon_{xx} + \sigma_{yy}\delta\varepsilon_{yy} + \tau_{xy}\delta\gamma_{xy} + \tau_{yz}\delta\gamma_{yz} + \tau_{xz}\delta\gamma_{xz}\right]d\Omega\,dz - \int_{\Omega} f_e\,\delta w d\Omega = 0 \quad (10)$$

Where Ω is the top surface of the plate, and is the density of the reaction force of the foundation.

For the Pasternak model:

$$f_e = k_w w - k_s \nabla^2 w \quad (11)$$

Or:

$\nabla^2 = \partial^2/\partial x^2 + \partial^2/\partial y^2$

w : Is the transverse displacement of the plate.

k_w : Is the module of the foundation of Winkler.

k_s : Is the stiffness of the Pasternak shear foundation layer.

Equilibrium equations are obtained from the principle of virtual works is:

$$N_{x,x} + N_{xy,y} = 0 \quad (12a)$$

$$N_{xy,x} + N_{y,y} = 0 \quad (12b)$$

$$\left(M^b_{x,xx} + 2M^b_{xy,xy} + M^b_{y,yy}\right) + N^0_x w_{,xx} + N^0_y w_{,yy} - k_w w + k_s \nabla^2 w = 0 \quad (12c)$$

$$\left(M^s_{x,xx} + 2M^s_{xy,xy} + M^S_{y,yy}\right) + Q_{yz,y} + Q_{xz,x} + N^0_x w_{,xx} + N^0_y w_{,yy} - k_w w + k_s \nabla^2 w = 0 \quad (12d)$$

Where the resulting forces and moments $(N, Q, S\ et\ M)$ of the P-FGM plate are determined by:

$$\left(N_i, M^b_i, M^s_i\right) = \int_{-\frac{h}{2}}^{\frac{h}{2}} \sigma_i \left(1, z, f(z)\right) dz, \quad (i = x, y, xy) \quad (13a)$$

$$Q_i = \int_{-h/2}^{h/2} \sigma_j \ f(z) dz, \quad (i = x, y), (j = xz, yz) \quad (13b)$$

Where:

$$N^0_x = N^0_y = \int_{-h/2}^{h/2} \frac{E(z)}{1-\nu} \alpha(z) T dz \quad (13c)$$

By substituting equation (4) in equation (13a) and integration with respect to the thickness of the plate, the results of the stresses are given as follows:

$$\begin{Bmatrix} N \\ M^b \\ M^s \end{Bmatrix} = \begin{bmatrix} A & B & C \\ B & D & D^s \\ C & D^s & F^s \end{bmatrix} \begin{Bmatrix} \varepsilon \\ k^b \\ k^s \end{Bmatrix}, \ Q_{ij} = A^s \gamma, \ i, j = x, y, xy \quad (14)$$

Where:

$$N = \left\{N_{xx}, N_{yy}, N_{xy}\right\}^t, \quad M^b = \left\{M^b_{xx}, M^b_{yy}, M^b_{xy}\right\}^t,$$

$$M^s = \left\{M^s_{xx}, M^s_{yy}, M^s_{xy}\right\}^t \quad (15)$$

$$\varepsilon = \left\{\varepsilon^0_{xx}, \varepsilon^0_{yy}, \gamma^0_{xy}\right\}^t, \quad k^b = \left\{k^b_{xx}, k^b_{yy}, k^b_{xy}\right\}^t,$$

$$k^s = \left\{k^s_{xx}, k^s_{yy}, k^s_{xy}\right\}^t \quad (16)$$

$$A = \begin{bmatrix} A_{11} & A_{12} & 0 \\ A_{12} & A_{22} & 0 \\ 0 & 0 & A_{33} \end{bmatrix}, \ B = \begin{bmatrix} B_{11} & B_{12} & 0 \\ B_{12} & B_{22} & 0 \\ 0 & 0 & B_{33} \end{bmatrix},$$

$$C = \begin{bmatrix} C_{11} & C_{12} & 0 \\ C_{12} & C_{22} & 0 \\ 0 & 0 & C_{33} \end{bmatrix} \quad (17)$$

$$D = \begin{bmatrix} D_{11} & D_{12} & 0 \\ D_{12} & D_{22} & 0 \\ 0 & 0 & D_{33} \end{bmatrix}, \ D^S = \begin{bmatrix} D^S_{11} & D^S_{12} & 0 \\ D^S_{12} & D^S_{22} & 0 \\ 0 & 0 & D^S_{33} \end{bmatrix},$$

$$F^S = \begin{bmatrix} F^S_{11} & F^S_{12} & 0 \\ F^S_{12} & F^S_{22} & 0 \\ 0 & 0 & F^a_{33} \end{bmatrix} \quad (18)$$

$$Q_{ij} = \left\{Q_{yz}, Q_{xz}\right\}^t, \ \gamma = \left\{\gamma^0_{xz}, \gamma^0_{yz}\right\}, \ A^S = \begin{bmatrix} A^S_{44} & 0 \\ 0 & A^S_{55} \end{bmatrix} \quad (19)$$

$$\left(A_{ij}, B_{ij}, C_{ij}, D, D^S_{ij}, F^S_{ij}\right) = \int_{-h/2}^{h/2} Q_{ij} \left(1, z, f(z), z^2, z f(z), f(z)^2\right) dz \quad (20)$$

$$A^S_{ij} = \int_{-h/2}^{h/2} Q_{ij} g(z)^2 dz, \ (i, j = 4,5) \quad (21)$$

$$N^0_x = N^0_y = \int_{-\frac{h}{2}}^{\frac{h}{2}} \frac{E(z)}{(1-\nu)} \alpha(z) T(z) dz \quad (22)$$

V. The exact solution for FGM plates

Rectangular plates are generally classified according to the type of substrate used. We consider here the exact solution for an FGM plate simply supported. Following the Navier solution procedure, we assume that the form of a following solution for u, v, w_b, w_s satisfies the boundary conditions:

$$\begin{Bmatrix} u \\ v \\ w_b \\ w_s \end{Bmatrix} = \begin{Bmatrix} U \cos(\lambda x) \sin(\mu y) \\ V \sin(\lambda x) \cos(\mu y) \\ W_b \sin(\lambda x) \sin(\mu y) \\ W_s \sin(\lambda x) \sin(\mu y) \end{Bmatrix} \quad (23)$$

Where: U, V, W_b, W_s are arbitrary parameters to be determined under the condition that the solution of equation (23) satisfies the equilibrium equations (12). The following equation is obtained:. $[K]\{\Delta\} = 0$

With $\{\Delta\} = \{U, V, W_b, W_s\}^t$ and $[C]$ is the symmetric matrix given by:

$$[K]=\begin{bmatrix} c_{11} & c_{12} & c_{13} & c_{14} \\ c_{12} & c_{22} & c_{23} & c_{24} \\ c_{13} & c_{23} & c_{33} & c_{34} \\ c_{14} & c_{24} & c_{34} & c_{44} \end{bmatrix} \quad (24)$$

In which:

$$\begin{aligned}
c_{11} &= -\left(A_{11}\lambda^2 + A_{66}\mu^2\right) \\
c_{12} &= -\lambda\,\mu\left(A_{12} + A_{66}\right) \\
c_{13} &= \lambda\left[B_{11}\lambda^2 + (B_{12} + 2B_{66})\,\mu^2\right] \\
c_{14} &= \lambda\left[C_{11}\lambda^2 + (C_{12} + 2C_{66})\,\mu^2\right] \\
c_{22} &= -\left(A_{66}\lambda^2 + A_{22}\mu^2\right) \\
c_{23} &= \mu\left[(B_{12} + 2B_{66})\,\lambda^2 + B_{22}\mu^2\right] \\
c_{24} &= \mu\left[C_{22}\mu^2 + (C_{12} + C_{66})\lambda^2\right] \\
c_{33} &= -\begin{pmatrix} D_{11}\lambda^4 + 2(D_{12} + 2D_{66})\lambda^2\mu^2 - D_{22}\mu^4 \\ + k_w + k_s(\mu^2 + \lambda^2) + N_y^0\mu^2 + N_x^0\lambda^2 \end{pmatrix} \\
c_{34} &= -\lambda\left(D_{11}^s\lambda^3 + 2(D_{12}^s + 2D_{66}^s)\,\mu^2\right) - D_{22}^s\mu^4 \\
&\quad - k_w - k_s(\mu^2 + \lambda^2) - N_y^0\mu^2 - N_x^0\lambda^2 \\
c_{44} &= -\lambda^2(F_{11}^a\lambda^2 + 2(2F_{66}^s + F_{12}^s)\mu^2 + N_x^0 + A_{55}^s - k_s) \\
&\quad - (N_y^0 + A_{44}^s + k_s)\mu^2 - F_{22}^s\mu^4 - k_w
\end{aligned} \quad (25)$$

V.1. uniform temperature rise(UTR)

It is assumed that the uniform initial temperature of the FGM plate is T_i, this temperature varies uniformly up to a final value T_f such that the plate flames. Therefore, (R. Javaheri and M. R. Eslami [20]), (H. Yaghoobi, A. Fereidoon, and R. Shahsiah [21]):

$$T(z) = T_f - T_i = \Delta T \quad (26)$$

V.2. Linear Temperature Distribution(LTD)

As a first approximation, consider the linear temperature distribution across the thickness as (M. Bodaghi and A. R. Saidi [22]):

$$T(z) = \frac{\Delta T}{h}\left(z + \frac{h}{2}\right) + T_m\,, \qquad \Delta T = T_c - T_m \quad (27)$$

V.3. Nonlinear Temperature Distribution(NTD)

The temperature field is assumed to be non-linear over the entire surface of the plate but varies along the direction of thickness due to thermal conduction. In this case, the distribution of temperatures along the thickness can be obtained by solving the following heat transfer equation (M. Bodaghi and A. R. Saidi [22]):

$$\frac{d}{dz}\left(K(z)\frac{d\,T(z)}{dz}\right) = 0\,,\ \ T\left(\frac{h}{2}\right) = T_c$$
$$et\ T\left(-\frac{h}{2}\right) = T_m \quad (28)$$

The Eq. (28) can be easily solved using the polynomial series. Thus, the temperature distribution across the thickness of the plate is obtained in the following form:

$$T(z) = T_m + \left(\frac{1}{2} + \frac{z}{h}\right)\Delta T\,\frac{\sum_{i=0}^{\infty}\left(\frac{1}{P\,i+1}\left(\frac{(K_m - K_c)\left(\frac{1}{2} + \frac{z}{h}\right)^P}{K_m}\right)^i\right)}{\sum_{i=0}^{\infty}\left(\frac{1}{P\,i+1}\left(\frac{(K_m - K_c)}{K_m}\right)^i\right)},$$
$$T = T_c - T_m \quad (29)$$

VI. Validation of results

To verify the accuracy of the present theory of FGM plates, comparisons are made between the results obtained from the current theory and those obtained by H. Yaghoobi and M. Torabi [23] as shown in the tables below. It can be seen that the current results are in good agreement with the results published for the FGM plates.

The following properties are considered as follows:

$$\boldsymbol{E_m = 70\ GPa\,,\nu_m = 0.3\,,\alpha_m = 23\times10^{-6}\ ^\circ C^{-1},K_m = 204\ W/mK}$$
$$\boldsymbol{E_c = 380\ GPa\,,\nu_c = 0.3\,,\alpha_c = 7.4\times10^{-6}\ ^\circ C^{-1},K_m = 10.4\ W/mK}$$

The temperature of the metal surface of the plate is assumed to be $\boldsymbol{T_m = 5\ ^\circ C}$

In addition, for all numerical results presented here, the values of the following variables are used, unless otherwise indicated in the tables or graphs.

$$\boldsymbol{\frac{a}{h} = 100, \qquad P = 5, \qquad K_w = K_s = 10.}$$

The dimensionless parameters of the elastic foundations of Winkler and Pasternak, as well as the critical buckling temperature difference, are used in the present analysis,

$$\boldsymbol{K_w = \frac{D_c\,k_w}{a^4}, \qquad K_s = \frac{D_c\,k_s}{a^2}, \qquad T_{cr} = 10^{-3}\,t_{cr}}$$

Where: $\boldsymbol{D_c = E_c\,h^3/[12(1-\upsilon^2)]}$

To verify the accuracy of the current solution, two particular cases are selected, which have been published as references in this area. Table

1 shows the difference in critical buckling temperature of the plate simply supported with b / h = 100.

Table 1: The critical buckling temperature difference of FGM plates without elastic foundation with b / h = 100.

	P	b/a=1		b/a=2		b/a=3		b/a=4		b/a=5	
		Present	**Réf [23]**	**Present**	**Réf [23]**	**Present**	**Réf [23]**	**Present**	**Réf [23]**	**Present**	**Réf [23]**
UTR	0	17.090	17.089	42.689	42.688	85.262	85.255	144.668	144.649	220.714	220.670
	1	7.940	7.940	19.837	19.836	39.627	39.625	67.258	67.251	102.653	102.636
	5	7.261	7.262	18.135	18.138	36.212	36.224	61.423	61.456	93.672	93.748
	10	7.464	7.464	18.639	18.643	37.209	37.225	63.093	63.138	96.178	96.282
LTD	0	24.179	24.179	75.378	75.375	160.523	160.510	279.336	279.298	431.429	431.341
	1	5.514	5.514	27.825	27.824	64.942	64.938	116.763	116.749	183.144	183.112
	5	3.892	3.893	22.609	22.614	53.725	53.745	97.120	97.177	152.630	152.762
	10	4.366	4.367	24.169	24.176	57.077	57.104	102.945	103.024	161.574	161.758
NTD	0	24.179	24.179	75.378	75.375	160.523	160.510	279.336	279.298	431.429	431.341
	1	7.654	7.654	38.624	38.623	90.146	90.139	162.078	162.058	254.221	254.177
	5	4.867	4.868	28.276	28.282	67.191	67.216	121.462	121.533	190.884	191.049
	10	5.046	5.047	27.934	27.942	65.969	66.000	118.983	119.074	186.745	186.958

Table 2: The critical buckling temperature difference of FGM plates with elastic foundation with b / h = 100.

P		a/h	UTR		LTD		NTD	
			Présente	Réf [23]	Présente	Réf [23]	Présente	Réf [23]
0	(0,0)	5	5.60962	5.58069	11.2092	11.15138	11.2092	11.15138
		10	1.621	1.61862	3.232	3.22725	3.232	3.22725
		20	0.42169	0.42153	0.83339	0.83307	0.83339	0.83307
	(10,0)	5	5.78516	5.75623	11.5603	11.50246	11.5603	11.50246
		10	1.66489	1.66251	3.31977	3.31502	3.31977	3.31502
		20	0.43267	0.43251	0.85533	0.85501	0.85533	0.85501
	(10,10)	5	9.25016	9.22123	18.4903	18.43246	18.4903	18.43246
		10	2.53114	2.52876	5.05227	5.04752	5.05227	5.04752
		20	0.64923	0.64907	1.28846	1.28814	1.28846	1.28814
5	(0,0)	5	2.31241	2.35948	3.97173	4.05274	4.9672	5.06851
		10	0.6827	0.68678	1.16652	1.17354	1.4589	1.46768
		20	0.17877	0.17905	0.29911	0.29959	0.37408	0.37468
	(10,0)	5	2.53919	2.58625	4.36208	4.44308	5.45538	5.55669
		10	0.7394	0.74347	1.26411	1.27113	1.58094	1.58972
		20	0.19294	0.19322	0.32351	0.32399	0.40459	0.40519
	(10,10)	5	7.01551	7.06257	12.0671	12.14814	15.0916	15.19291

		10	1.85848	1.86255	3.19037	3.19739	3.99	3.99878
		20	0.47271	0.47299	0.80507	0.80555	1.00685	1.00745
10	(0,0)	5	2.3076	2.36822	4.08035	4.18778	4.71603	4.8402
		10	0.69563	0.70108	1.22384	1.2335	1.4145	1.42567
		20	0.18335	0.18373	0.31605	0.31672	0.36529	0.36606
	(10,0)	5	2.56354	2.62416	4.53389	4.64132	5.24023	5.3644
		10	0.75961	0.76507	1.33722	1.34688	1.54555	1.55672
		20	0.19935	0.19972	0.3444	0.34506	0.39805	0.39882
	(10,10)	5	7.61563	7.67626	13.4865	13.59396	15.5876	15.71178
		10	2.02264	2.02809	3.57538	3.58504	4.13239	4.14356
		20	0.5151	0.51548	0.90394	0.9046	1.04476	1.04553

Table 3: The critical buckling temperature difference of FGM plates under uniform temperature rise.

P	a/b	a/h	Present	Réf [23]
0	0.5	40	125.17972	125.1757
		60	55.67066	55.6699
		80	31.32169	31.3214
		100	20.04794	20.0478
	1	40	163.38773	163.3775
		60	72.70680	72.7048
		80	40.91534	40.9147
		100	26.19109	26.1908
	2	40	320.14075	320.0775
		60	142.84328	142.8307
		80	80.46001	80.4560
		100	51.52727	51.5256
5	0.5	40	103.92242	103.9294
		60	46.20527	46.2067
		80	25.99393	25.9944
		100	16.63714	16.6373
	1	40	118.71483	118.7327
		60	52.80693	52.8105
		80	29.71274	29.7139
		100	19.01878	19.0192
	2	40	183.75782	183.8681
		60	81.94761	81.9696
		80	46.15057	46.1576
		100	29.55272	29.5556
10	0.5	40	114.43056	114.4401
		60	50.87870	50.8806
		80	28.62335	28.6239
		100	18.32015	18.3204
	1	40	129.40681	129.4310
		60	57.56693	57.5717
		80	32.39183	32.3933
		100	20.73386	20.7345
	2	40	195.91621	196.0656
		60	87.40054	87.4304
		80	49.22767	49.2372
		100	31.52499	31.5289

Table 4: The critical buckling temperature difference of FGM plates under linear temperature distribution.

P	a/b	a/h	Present	Réf [23]
0	0.5	40	240.3594	240.3514
		60	101.3413	101.3397
		80	52.6434	52.6429
		100	30.0959	30.0957
	1	40	316.7755	316.7550
		60	135.4136	135.4095
		80	71.8307	71.8294
		100	42.3822	42.3817
	2	40	630.2815	630.1551
		60	275.6866	275.6614
		80	150.9200	150.9120
		100	93.0545	93.0513
5	0.5	40	212.9515	212.9666
		60	88.7031	88.7061
		80	45.1939	45.1948
		100	25.0514	25.0518
	1	40	244.7954	244.8338
		60	102.9146	102.9222
		80	53.1994	53.2018
		100	30.1784	30.1794
	2	40	384.8142	385.0516
		60	165.6461	165.6935
		80	88.5853	88.6004
		100	52.8549	52.8611
10	0.5	40	224.1286	224.1481
		60	93.9658	93.9697
		80	48.3838	48.3850
		100	27.2815	27.2820
	1	40	254.8020	254.8516
		60	107.6642	107.6740
		80	56.1022	56.1053
		100	32.2251	32.2264
	2	40	391.0223	391.3282
		60	168.7675	168.8286
		80	90.5843	90.6037
		100	54.3268	54.3348

Table 5: The critical buckling temperature difference of FGM plates under nonlinear temperature distribution.

P	a/b	a/h	Present	Réf [23]
0	0.5	40	240.3594	240.3514
		60	101.3413	101.3397
		80	52.6434	52.6429
		100	30.0959	30.0957
	1	40	316.7755	316.7550
		60	135.4136	135.4095
		80	71.8307	71.8294
		100	42.3822	42.3817
	2	40	630.2815	630.1551
		60	275.6866	275.6614
		80	150.9200	150.9120
		100	93.0545	93.0513
5	0.5	40	212.9515	212.9666
		60	88.7031	88.7061
		80	45.1939	45.1948
		100	25.0514	25.0518
	1	40	244.7954	244.8338
		60	102.9146	102.9222
		80	53.1994	53.2018

		100	30.1784	30.1794
	2	40	384.8142	385.0516
		60	165.6461	165.6935
		80	88.5853	88.6004
		100	52.8549	52.8611
	0.5	40	224.1286	224.1481
		60	93.9658	93.9697
		80	48.3838	48.3850
		100	27.2815	27.2820
	1	40	254.8020	254.8516
10		60	107.6642	107.6740
		80	56.1022	56.1053
		100	32.2251	32.2264
	2	40	391.0223	391.3282
		60	168.7675	168.8286
		80	90.5843	90.6037
		100	54.3268	54.3348

Table 6: The effects of elastic foundation on the critical buckling temperature difference of FGM plates.

	k_s	k_w	Present	Réf [23]
UTR	10	10	19.0188	19.0192
		50	63.7820	63.7824
		100	119.7360	119.7364
	100	10	24.1212	24.1216
		50	68.8844	68.8848
		100	124.8383	124.8388
	1000	10	52.0032	52.0061
		50	96.7664	96.7693
		100	152.7204	152.7233
LTD	10	10	24.1304	24.1312
		50	101.1809	101.1817
		100	197.4941	197.4949
	100	10	32.9131	32.9139
		50	109.9636	109.9644
		100	206.2768	206.2776
	1000	10	80.9063	80.9112
		50	157.9568	157.9618
		100	254.2700	254.2749
NTD	10	10	30.1784	30.1794
		50	126.5407	126.5417
		100	246.9935	246.9945
	100	10	41.1624	41.1634
		50	137.5247	137.5257
		100	257.9775	257.9785
	1000	10	101.1845	101.1906
		50	197.5467	197.5529
		100	317.9996	318.0058

Table 2 shows a very good agreement can be seen between our results and that of literature published previously.

The effects of the aspect ratio of the plate, the side-to-thickness ratio and the power index over the critical buckling temperature difference of the plate under a uniform, Linaire and non-linear distribution are listed in Tables 3 , 4 and 5, respectively.

After validations, we discuss the influence of elastic foundation parameters on the critical buckling temperature (T_{cr}) of the FGM plates under three types of thermal loads (Table 6).

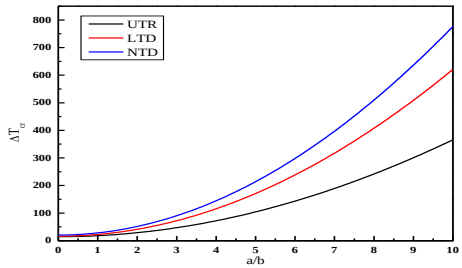

Fig.: 1: The aspect ratio effects a / b on the buckling critical temperature difference (Tcr) of FGM plates under uniform, linear and nonlinear temperature distribution.

FIG. 2 illustrates the a / b ratio effect for a plate simply supported on the critical buckling temperature (T_{cr}) of the FGM plates under a uniform, linear and non-linear temperature distribution. It can be seen that if, by increasing the value of a / b, the deformation due to the buckling requires a high temperature, the buckling of the plate. Moreover, it appears from this figure that the variation (T_{cr}) is more progressive than when a simply supported plate adopted as a limit condition.

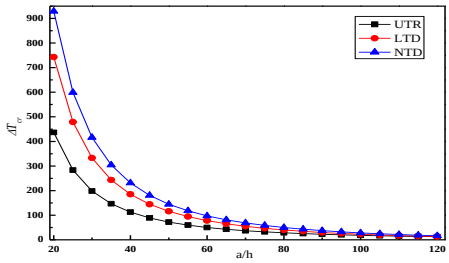

Fig.: 3: The side-to-thickness ratio effect a/h on the buckling critical temperature difference (Tcr) of FGM plates under uniform, linear and nonlinear temperature distribution.

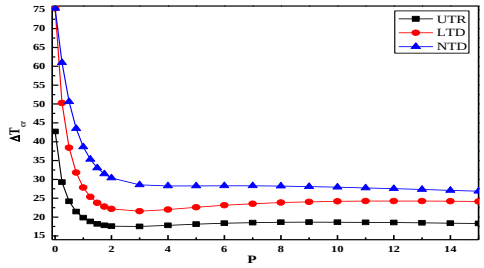

Fig.: 4: The power-law index effect P on the buckling critical temperature difference (Tcr) of FGM plates under uniform, linear and nonlinear temperature distribution.

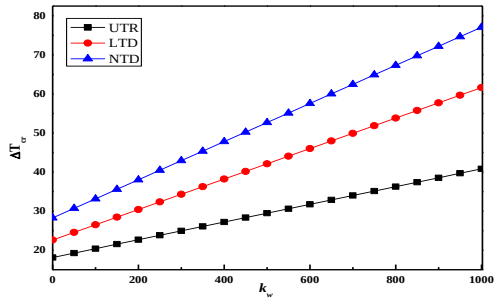

Fig.: 5: The transverse springiness coefficient (kw) on the buckling critical temperature difference (Tcr) of FGM plates under uniform, linear and nonlinear temperature distribution.

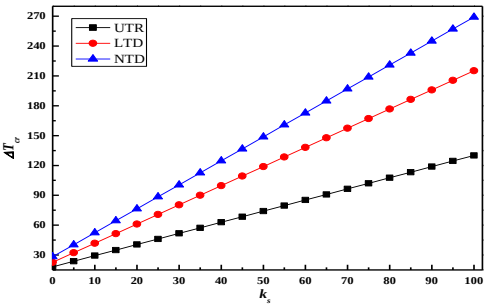

Fig.: 6: The shear stiffness coefficient (ks) on the buckling critical temperature difference (Tcr) of FGM plates under uniform, linear and nonlinear temperature distribution.

VII. Conclusions

The study and thermal buckling analysis of FGM plates under a uniform, linear and nonlinear distribution of thermal loading across the thickness using the theory of the hyperbolic shear deformation plate are presented. The present problem is analyzed when the FGM plates are based on two parameters (Pasternak model) of the elastic foundations. The constituent materials are classified according to the variation of the power law across the thickness only. The results obtained by the present theory are compared with those

obtained by H. YAGHOOBI and AL. The following conclusions can be drawn from this study:

• To show the accuracy of the current results, the convergence of the numerical solution was examined. It is found that the results presented are very consistent with these being in the literature.

• The critical buckling temperature decreases as the aspect ratio increases.

• The results show that the presence of elastic foundations leads to a significant increment in the variation of critical buckling temperature difference.

Finally, we hope that this study will serve as a basis for future civil engineering researchers to develop and deepen their knowledge in the field of use of gradient properties (FGM) materials, isotropic, orthotropic, sandwich materials to civilian needs.

References

[1] Wu.L, «Thermal buckling of a simply supported moderately thick rectangular FGM plate,» *Compos. Struct., vol. 64, pp. 211-218, 2004*.

[2] Woo.J et al, «Thermomechanical postbuckling analysis of moderately thick functionally graded plates and shallow shells,» *J. Mech. Sci., vol. 47, n° %18, pp. 1147-1171, 2005.*

[3] Prakash.T et al, «Thermal postbuckling analysis of FGM skew plates,» *Ing. Struct, vol. 30, pp. 22-32, 2008.*

[4] Matsunaga.H, «Thermal buckling of functionally graded plates according to a 2D higher-order deformation theory,» *Compos. Struct., vol. 90, pp. 76-86, 2009.*

[5] Shahrjerdi.A, Mustapha.F, Bayat.M and Majid.D.L.A, «Free vibration analysis of solar functionally graded plates with temperature-dependent material properties using second order shear deformation theory,» *Mech. Sci. Tech, vol. 25, n° %19, pp. 2195-2209, 2007.*

[6] Tounsi.A, Benguediab.S, Adda Bedia.E.A, Semmah.A et and Zidour. M, «Nonlocal effects on thermal buckling properties of double-walled carbon nanotubes,» *Adv. Nano Res, vol. 1, n° %11, pp. 1-11, 2013.*

[7] Bouderba.B, Houari.M.S.A, and Tounsi.A, «Thermomechanical bending response of FGM thick plates resting on Winkler-Pasternak elastic foundations,» *Steel Compos. Struct, vol. 14, n° %11, pp. 85-104, 2013.*

[8] Golmakani, M.E., «Large deflection thermoelastic analysis of shear deformable functionally graded variable thickness rotating disk,» *Compos. Part B, vol. 45, pp. 1143-1155, 2013.*

[9] Chakraverty, S. and Pradhan, K.K., «Free vibration of exponential functionally graded rectangular plates in thermal environment with general boundary conditions,» *Aerosp. Sci. Tech, vol. 36, pp. 132-156, 2014a.*

[10] Chakraverty, S. and Pradhan, K.K., «Free vibration of functionally graded thin rectangular plates resting on Winkler elastic foundation with general boundary conditions using Rayleigh-Ritz method,» *Aerosp. Sci. Tech, vol. 36, pp. 132-156, 2014b.*

[11] Zidi.M, Tounsi. A, Houari M.S.A, Adda Bedia E.A et and Anwar Bég. O, «Bending analysis of FGM plates under hygro-thermo-mechanical loading using a four variable refined plate theory,» *Aerosp. Sci. Tech, vol. 34, pp. 24-34, 2014.*

[12] Belabed, Z., Houari, M.S.A., Tounsi, A., Mahmoud,S et .R. and Anwar Bég, O., «An efficient and simple higher order shear and normal deformation theory for functionally graded material (FGM) plates,» *Compos. Part B, vol. 60, pp. 274-283, 2014.*

[13] Bousahla, A.A., Houari, M.S.A., Tounsi, A. and et Adda Bedia, E.A, «A novel higher order shear and normal deformation theory based on neutral surface position for bending analysis of advanced composite plates,» *J. Comput. Meth, vol. 11, n° %16, 2014.*

[14] Hebali Habib, Tounsi. A, Houari M.S.A, Bessaim. A, et Adda Bedia E.A, «New Quasi-3D Hyperbolic Shear Deformation Theory for the Static and Free Vibration Analysis of Functionally Graded Plates,» *J. Eng. Mech., pp. 374-383, 2014.*

[15] Mantari, J.L. and Granados, E.V., «Thermoelastic behavior of advanced composite sandwich plates by using a new 6 unknown quasi-3D hybrid type HSDT,» *Compos. Struct, vol. 126, pp. 132-144, 2015.*

[16] Pradhan, K.K. and Chakraverty, S., «Static analysis of functionally graded thin rectangular plates with various boundary supports,» *Arch. Civil Mech. Eng, vol. 15, n° %13, pp. 721-734, 2015c.*

[17] Rad, A.B., «Thermo-elastic analysis of functionally graded circular plates resting on a gradient hybrid foundation,» *Appl. Math. Comput, vol. 256, pp. 276-298, 2015.*

[18] Mahi, A., Adda Bedia, E.A. and Tounsi, A., «A new hyperbolic shear deformation theory for bending and free vibration analysis of isotropic, functionally graded, sandwich and laminated composite plates,» *Appl. Math. Model, vol. 39, pp. 2489-2508, 2015.*

[19] Chikh, Abdelbaki,, Ahmed Bakora, Houari Heireche,, Mohammed Sid Ahmed Houari, Abdelouahed Tounsi et and E.A. Adda Bedia, «Thermo-mechanical postbuckling of symmetric S-FGM plates resting on Pasternak elastic foundations using hyperbolic shear deformation theory,» *Structural Engineering and Mechanics, vol. 04, n° %157, pp. 617-639, 2016.*

[20] R. Javaheri and M. R. Eslami, «Thermal Buckling of Functionally Graded Plates Bases on Higher Order Theory,» *Therm Stresses, vol. 25, pp. 603-625, 2002.*

[21] H. Yaghoobi, A. Fereidoon, and R. Shahsiah,, «Thermal Buckling of Axially Functionally Graded Thin Cylindrical Shell,» *Therm Stresses, vol. 34, pp. 1520-1270, 2011.*

[22] M. Bodaghi, and A. R. Saidi, «Thermoelastic Buckling Behavior of Thick Functionally Graded Rectangular Plates,» *Arch Appl Mech, vol. 81, pp. 1555-1572, 2011.*

[23] Hessameddin Yaghoobi, Mohsen Torabi, «Exact Solution for Thermal Buckling of Functionally Graded Plates Resting on Elastic Foundations with Various Boundary Conditions,» *Thermal Stresses, vol. 36, n° %19, pp. 869-894, 2013.*